Supporting information

A chemical composition evolution for the shape-controlled synthesis and energy storage applicability of Fe_3O_4/C nanostructures

Fenfen Xu, Wenpei Kang, Xinxin Wang, Rui Liu, Chenhao Zhao and Qiang Shen[*]

(* Corresponding author, E-mail: qshen@sdu.edu.cn)

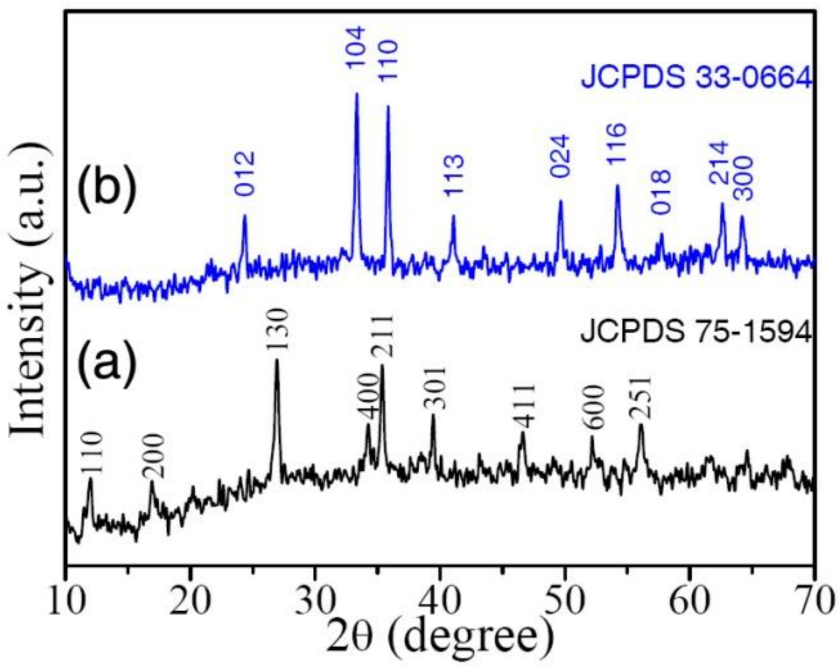

Fig.S1. XRD patterns of (a) solvothermal and (b) hydrothermal products obtained after a reaction time of 9 h, coinciding well with the crystal structures of rhombohedral hematite (α-Fe_2O_3, JCPDS 33-0664) and tetragonal akaganeite (β-FeOOH, JCPDS 75-1594), respectively.

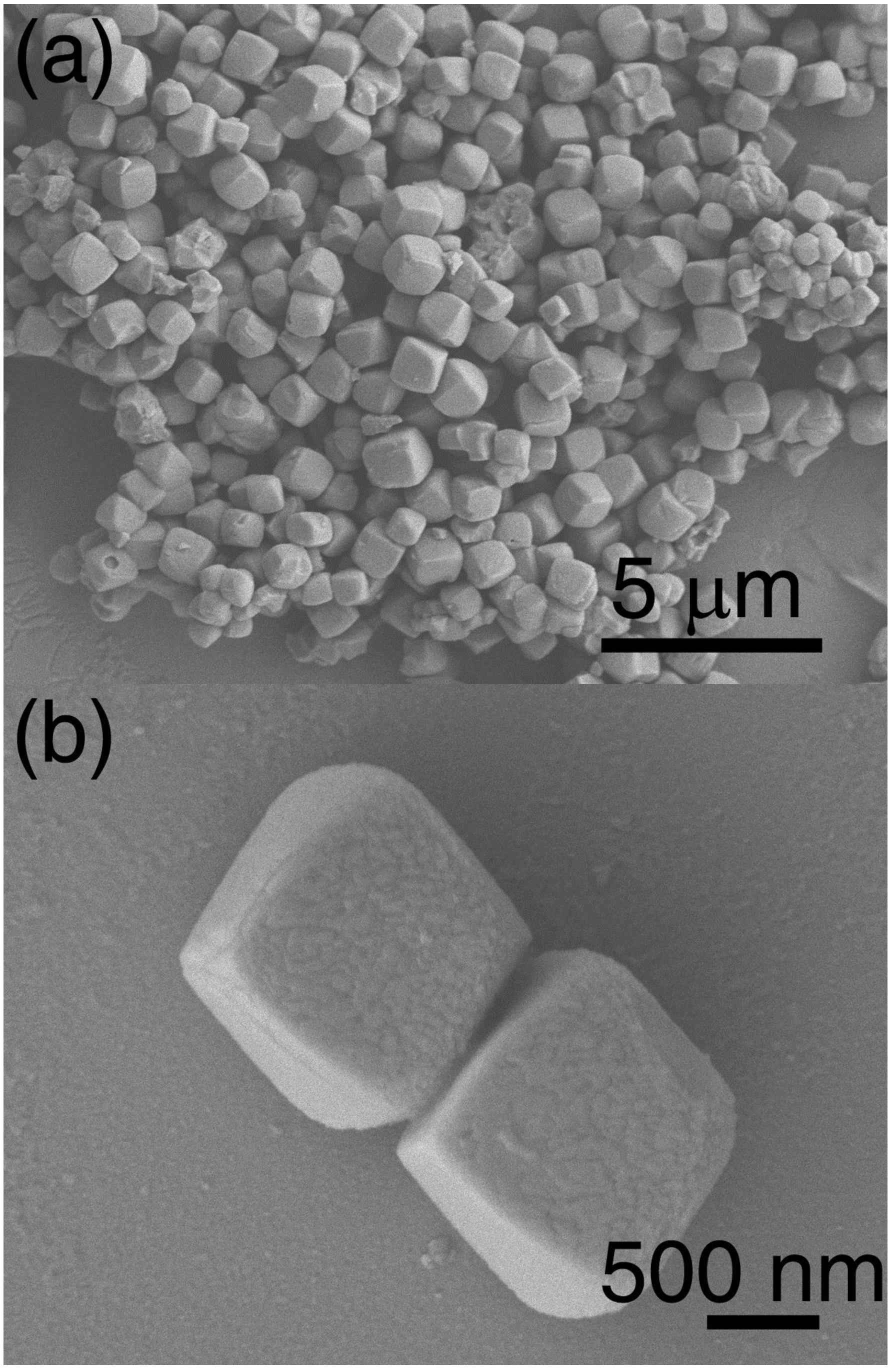

Fig.S2. SEM images of rhombohedral α-Fe_2O_3 obtained at the solvothermal reaction time of 9 h: (a) overall view; (b) close-up view.

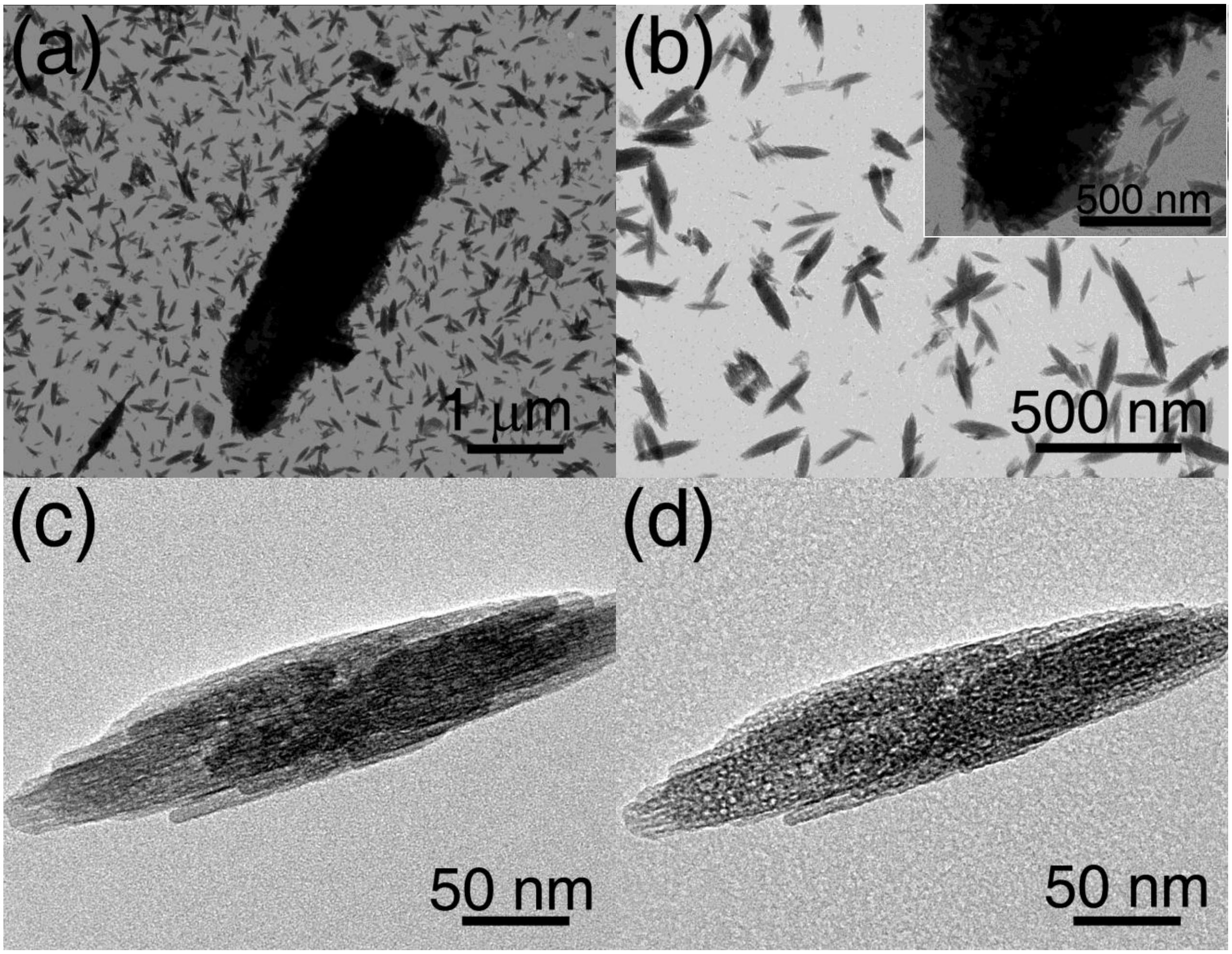

Fig.S3. (a, b) TEM images of as-prepared FeOCl nanospindles, the crystal structures of which are extremely unstable even under an air storage condition. Inset is the magnified TEM picture of the big "rod" in panel (a), showing that it is composed of spindles-like building blocks. (c, d) TEM images of a representative β-FeOOH nanospindle taken before and after a short-time irradiation of electron beam, respectively.

Crystalline β-FeOOH comes from the solution-mediated transformation of unstable FeOCl, which is indicative of a relatively stable nature of β-FeOOH therein. As shown in panels (c) and (d), the irradiation-induced dehydration of a β-FeOOH nanospindle indicates that the subsequent phase transformation of β-FeOOH to thermodynamically stable Fe_2O_3 (or Fe_3O_4) should be conducted under a relatively harsh experimental condition.

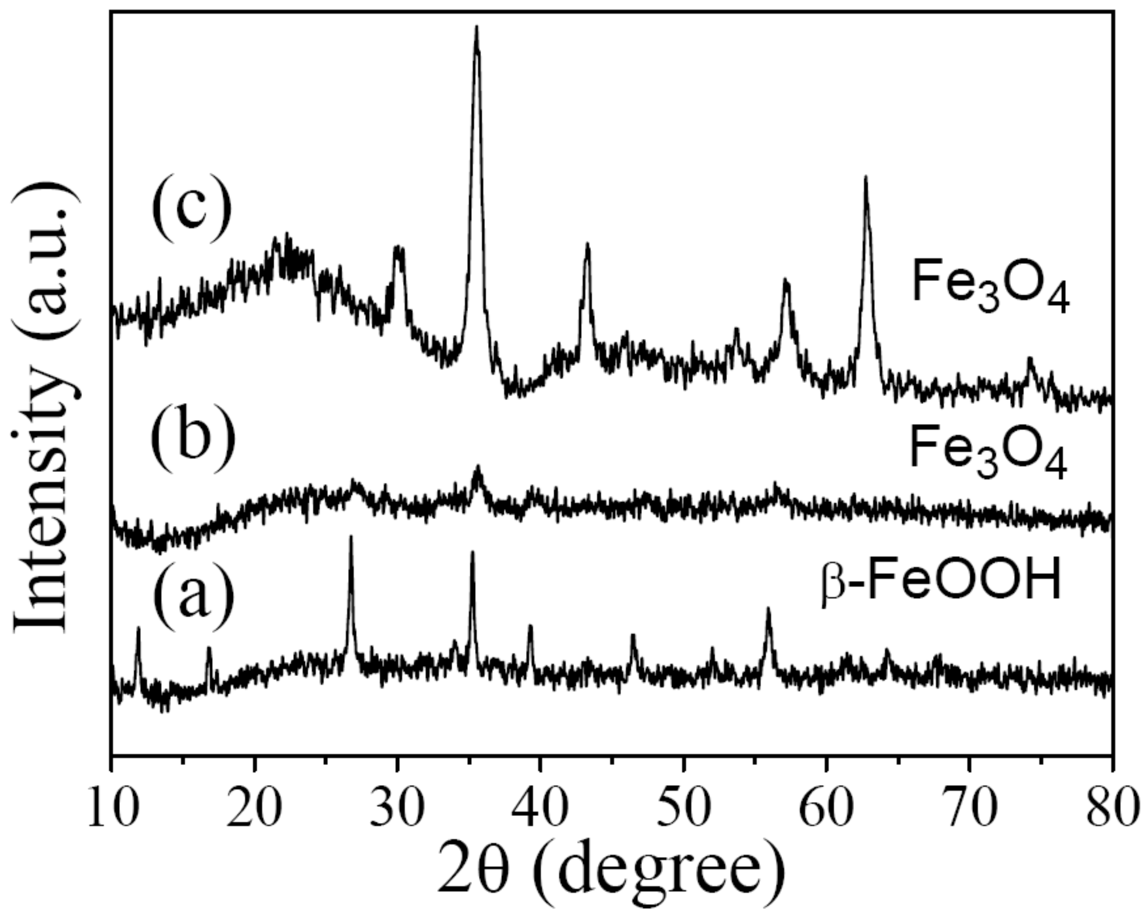

Fig.S4. XRD patterns of previously obtained spindle-like β-FeOOH and its subsequently treated products: (a) as-prepared β-FeOOH; (b) the initially formed Fe_3O_4 crystals after the solvothermal treatment of as-prepared β-FeOOH; (c) the final products of Fe_3O_4/C spindle-like nanocomposites.

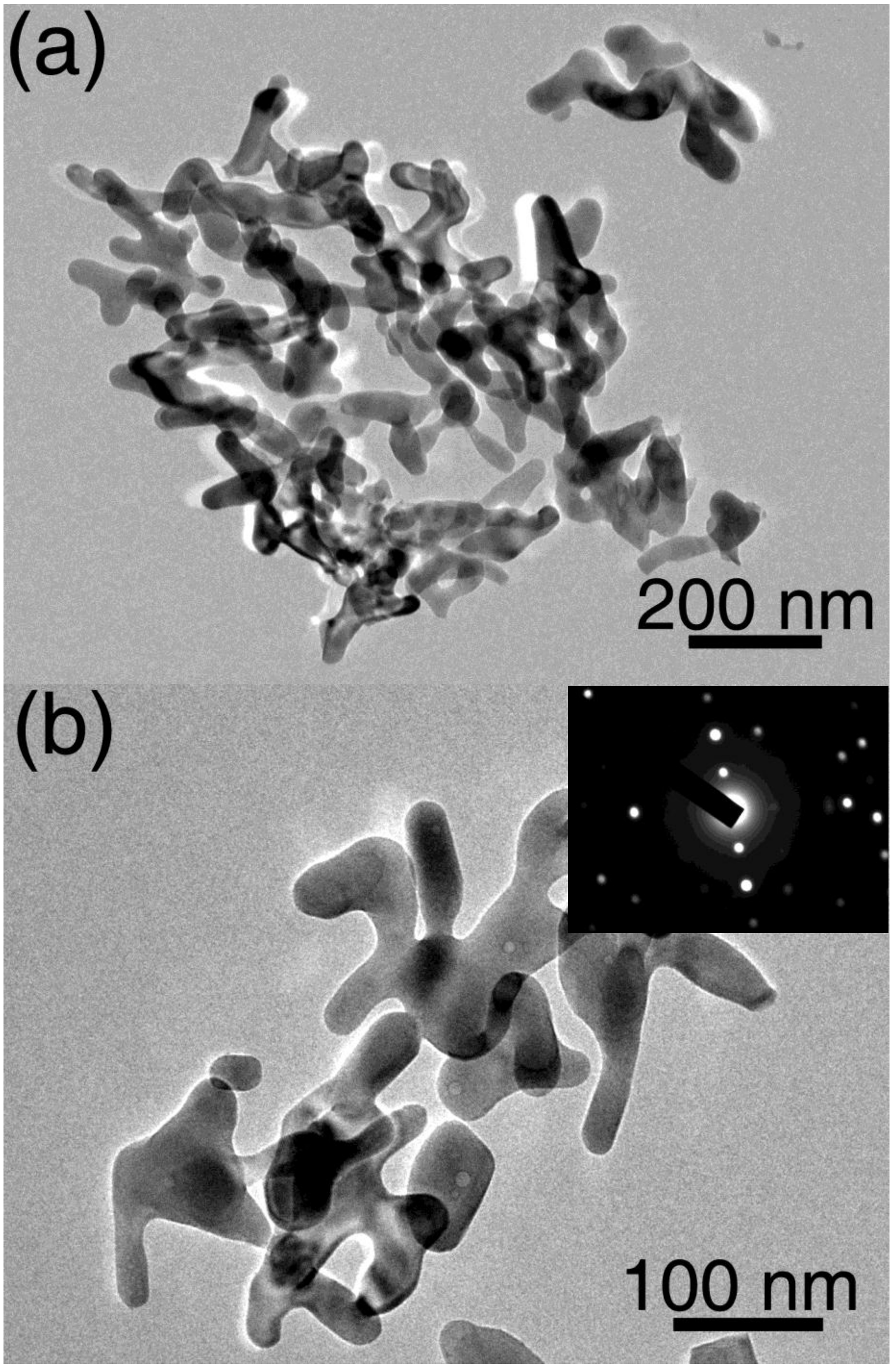

Fig.S5. TEM images of interconnected and irregular nanoparticles of α-Fe_2O_3 obtained after the heat-treatment of β-FeOOH nanospindles under air atmosphere: (a) overall view; (b) close-up view. Inset is the corresponding SAED pattern taken by focusing electron beam on these nanoparticles, showing a polycrystalline nature.

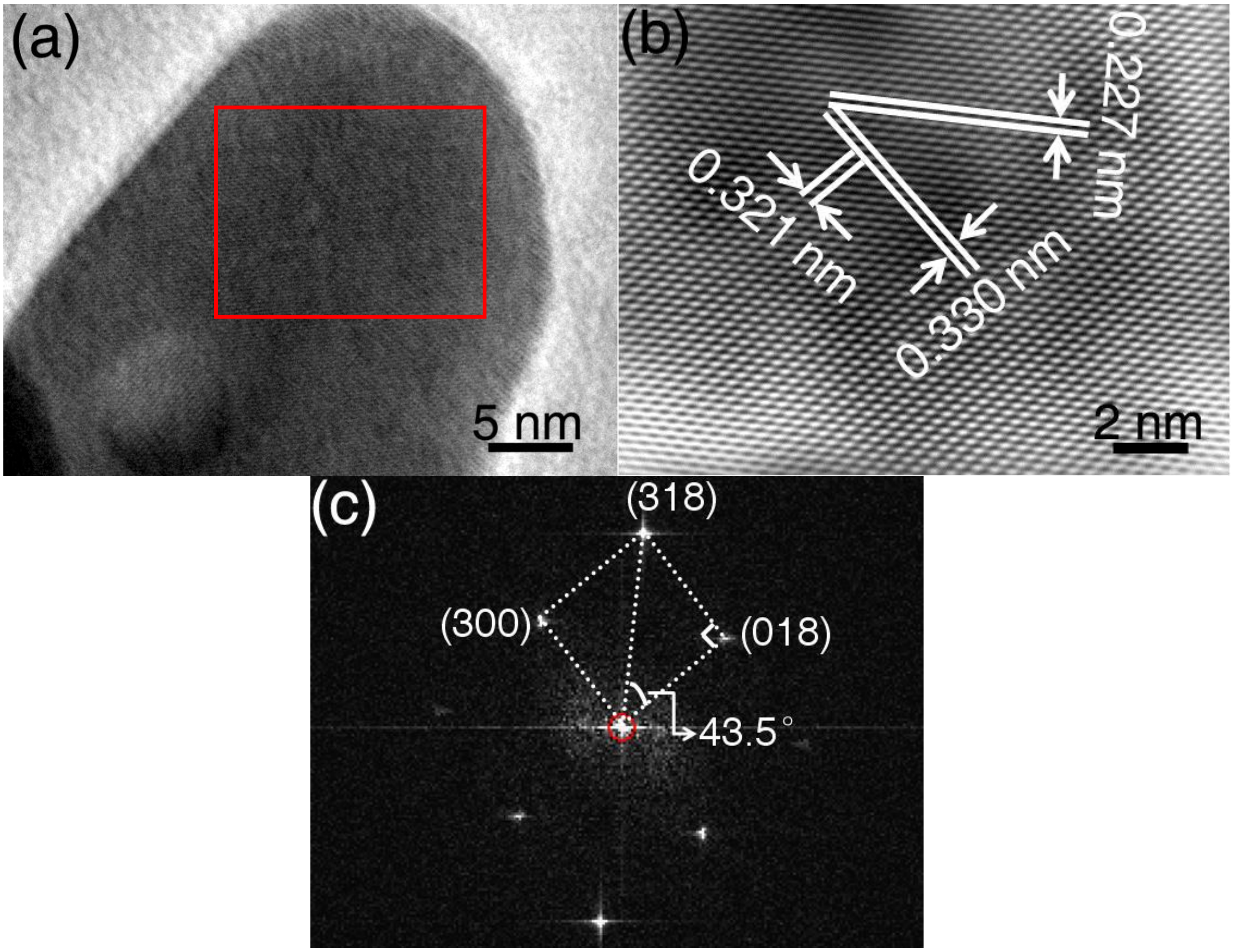

Fig.S6. (a) A representative HR TEM image of an irregular nanoparticle of α-Fe_2O_3 obtained after the heat-treatment of β-FeOOH nanospindles under air atmosphere, and a red rectangle region was selected shown in panels (b) and (c). (b) Filtered picture and (c) corresponding Fourier transform pattern of the red rectangle region show the lattice parameters of rhombohedral hematite along [0-81] zone axis, indicating a single-crystalline nature.

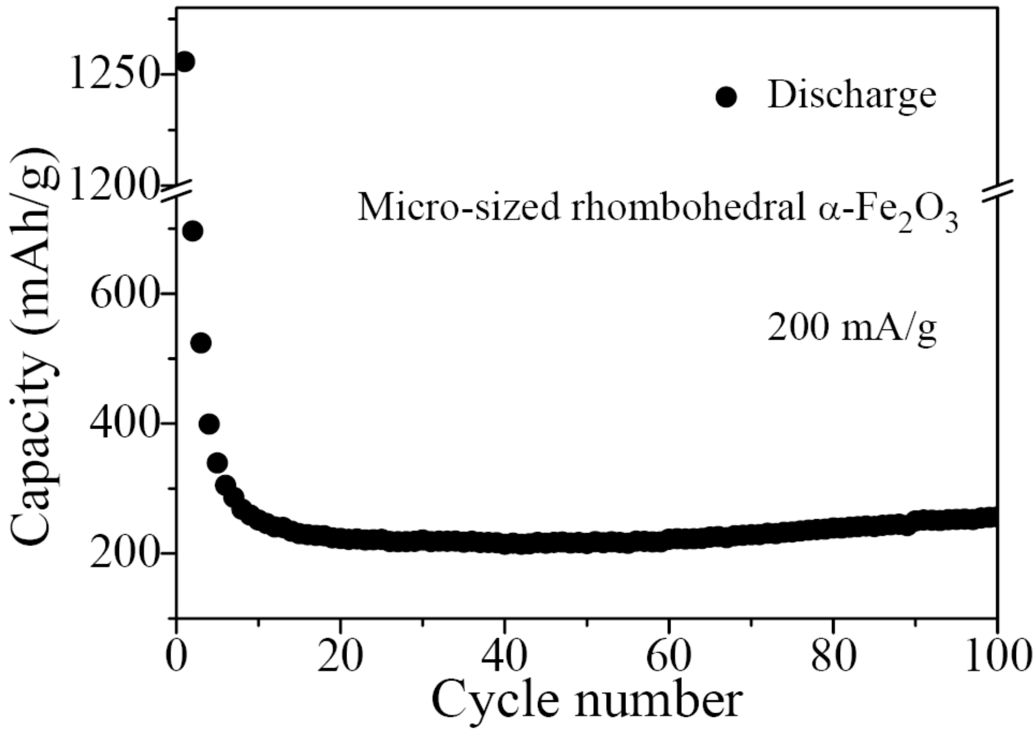

Fig.S7. A plot of the specific discharge capacity of a micro-sized α-Fe_2O_3 (Also seen *Fig.* S2) electrode against the cycle number of galvanostatic discharge-charge between 0.01 and 3.0 V at a current density of 200 mA/g.

For the 1st, 2nd and 100th discharge-charge cycles at 200 mA/g, the observed specific discharge capacities of a micro-sized α-Fe_2O_3 electrode are 1255.8, 696.4 and 256.4 mAh/g, respectively.

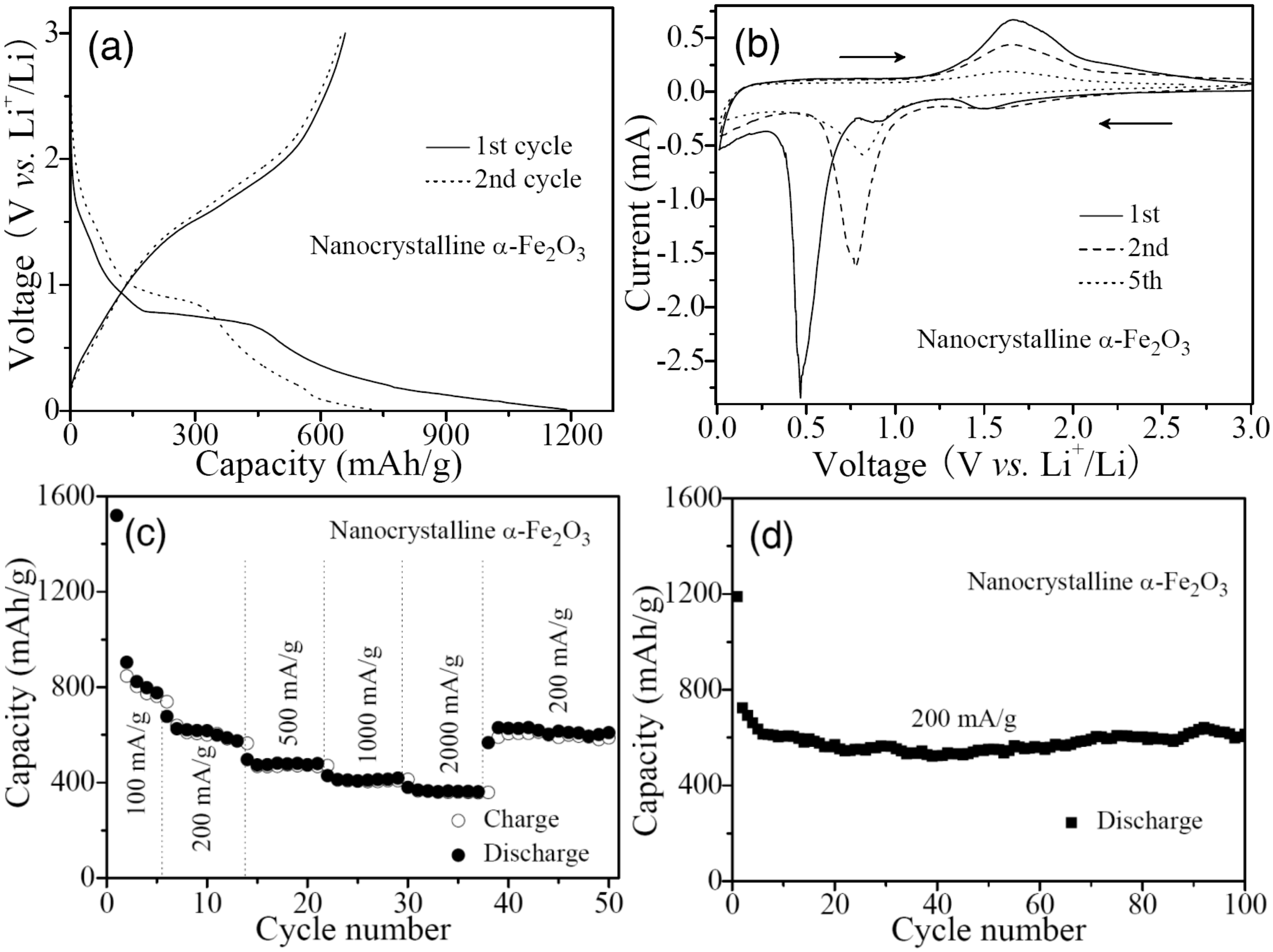

Fig.S8. Electrochemical behaviors of nanocrystalline α-Fe_2O_3 (Also seen *Fig.* S5 and S6) electrodes: (a) voltage profiles at a current rate of 200 mA/g; (b) CV curves at a scanning rate of 0.1 mV/s; (c) plots of specific capacity against cycle number at different current densities; (d) cycling stability at a charge-discharge current density of 200 mA/g.

For the 1^{st}, 2^{nd} and 100^{th} discharge-charge cycles at 200 mA/g, the observed specific discharge capacities of a nanocrystalline α-Fe_2O_3 electrode are 1189.1, 724.5 and 614.6 mAh/g, respectively. In comparison with the results shown in Fig. S7, nanocrystalline α-Fe_2O_3 electrode possesses the better cycling performance and/or the higher capacity retention, probably owing to its smaller average particle size.